

The Jackson Laboratory

The Mouseion at the JAXlibrary

Faculty Research 2020

Faculty Research

9-1-2020

Cross-Species Analyses Identify Dlgap2 as a Regulator of Age-Related Cognitive Decline and Alzheimer's Dementia.

Andrew R Ouellette

Sarah M Neuner

Logan Dumitrescu

Laura C. Anderson

Daniel M. Gatti

See next page for additional authors

Follow this and additional works at: <https://mouseion.jax.org/stfb2020>



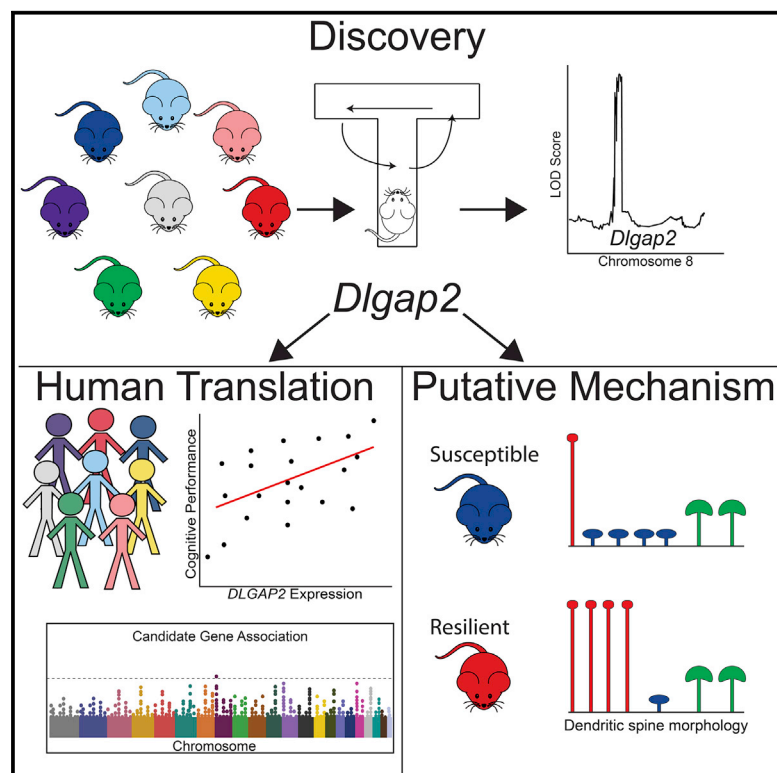
Part of the [Life Sciences Commons](#), and the [Medicine and Health Sciences Commons](#)

Authors

Andrew R Ouellette, Sarah M Neuner, Logan Dumitrescu, Laura C. Anderson, Daniel M. Gatti, Emily R Mahoney, Jason A. Bubier, Gary Churchill, Luanne L. Peters, Matthew J Huentelman, Jeremy H Herskowitz, Hyun-Sik Yang, Alexandra N Smith, Christiane Reitz, Brian W Kunkle, Charles C White, Philip L De Jager, Julie A Schneider, David A Bennett, Nicholas T Seyfried, Alzheimer's Disease Genetics Consortium, Elissa J Chesler, Niran Hadad, Timothy J Hohman, and Catherine Kaczorowski

Cross-Species Analyses Identify *Dlgap2* as a Regulator of Age-Related Cognitive Decline and Alzheimer's Dementia

Graphical Abstract



Authors

Andrew R. Ouellette, Sarah M. Neuner, Logan Dumitrescu, ..., Niran Hadad, Timothy J. Hohman, Catherine C. Kaczorowski

Correspondence

elissa.chesler@jax.org (E.J.C.), niran.hadad@jax.org (N.H.), timothy.j.hohman@vumc.org (T.J.H.), catherine.kaczorowski@jax.org (C.C.K.)

In Brief

Ouellette et al. identify *Dlgap2* as a potential modifier of working memory in an aged Diversity Outbred (DO) mouse population. The cross-species significance of this finding is highlighted by the association between human *DLGAP2* and Alzheimer's disease phenotypes at the variant, gene expression, and methylation levels.

Highlights

- *Dlgap2* QTL associates with working memory decline in Diversity Outbred (DO) mice
- *DLGAP2* variants associate with AD by GWAS in human populations
- *DLGAP2* gene and protein expression are associated with cognitive decline in humans
- Results highlight translational relevance of DO mice for studying complex traits



Report

Cross-Species Analyses Identify *Dlgap2* as a Regulator of Age-Related Cognitive Decline and Alzheimer's Dementia

Andrew R. Ouellette,^{1,2,16} Sarah M. Neuner,^{1,3,16} Logan Dumitrescu,^{4,5,16} Laura C. Anderson,¹ Daniel M. Gatti,¹ Emily R. Mahoney,⁴ Jason A. Bubier,¹ Gary Churchill,¹ Luanne Peters,¹ Matthew J. Huentelman,⁶ Jeremy H. Herskowitz,⁷ Hyun-Sik Yang,^{8,9,10} Alexandra N. Smith,⁴ Christiane Reitz,¹¹ Brian W. Kunkle,¹² Charles C. White,^{8,13} Philip L. De Jager,^{8,13} Julie A. Schneider,¹⁴ David A. Bennett,¹⁴ Nicholas T. Seyfried,¹⁵ Alzheimer's Disease Genetics Consortium, Elissa J. Chesler,^{1,17,*} Niran Hadad,^{1,17,*} Timothy J. Hohman,^{4,5,17,*} and Catherine C. Kaczorowski^{1,2,17,18,*}

¹The Jackson Laboratory, Bar Harbor, ME 04609, USA

²Graduate School of Biomedical Science and Engineering, The University of Maine, Orono, ME 04469, USA

³University of Tennessee Health Science Center, Memphis, TN 38163, USA

⁴Vanderbilt Memory and Alzheimer's Center, Department of Neurology, Vanderbilt University Medical Center, Nashville, TN 37240, USA

⁵Vanderbilt Genetics Institute, Vanderbilt University Medical Center, Nashville, TN 37240, USA

⁶Neurogenetics Division, Translational Genomics Research Institute, Phoenix, AZ 85004, USA

⁷Center for Neurodegeneration and Experimental Therapeutics and Department of Neurology, University of Alabama at Birmingham, Birmingham, AL 35294, USA

⁸Cell Circuits and Epigenomics Program, Broad Institute of MIT and Harvard, 415 Main Street, Cambridge, MA 02142, USA

⁹Department of Neurology, Massachusetts General Hospital, Harvard Medical School, Boston, MA 02114, USA

¹⁰Center for Alzheimer Research and Treatment, Department of Neurology, Brigham and Women's Hospital, Harvard Medical School, Boston, MA 02114, USA

¹¹Taub Institute for Research on Alzheimer's Disease and the Aging Brain, Gertrude H. Sergievsky Center, and Departments of Neurology and Epidemiology, College of Physicians and Surgeons, Columbia University, New York, NY 10032, USA

¹²Miller School of Medicine, University of Miami, Miami, FL 33136, USA

¹³Center for Translational and Computational Neuroimmunology, Department of Neurology, Columbia University Medical Center, New York, NY 10032, USA

¹⁴Rush Alzheimer's Disease Center, Rush University Medical Center, Chicago, IL 60612, USA

¹⁵Department of Biochemistry, Emory University School of Medicine, Atlanta, GA 30322, USA

¹⁶These authors contributed equally

¹⁷Senior author

¹⁸Lead Contact

*Correspondence: elissa.chesler@jax.org (E.J.C.), niran.hadad@jax.org (N.H.), timothy.j.hohman@vumc.org (T.J.H.), catherine.kaczorowski@jax.org (C.C.K.)

<https://doi.org/10.1016/j.celrep.2020.108091>

SUMMARY

Genetic mechanisms underlying age-related cognitive decline and dementia remain poorly understood. Here, we take advantage of the Diversity Outbred mouse population to utilize quantitative trait loci mapping and identify *Dlgap2* as a positional candidate responsible for modifying working memory decline. To evaluate the translational relevance of this finding, we utilize longitudinal cognitive measures from human patients, RNA expression from post-mortem brain tissue, data from a genome-wide association study (GWAS) of Alzheimer's dementia (AD), and GWAS results in African Americans. We find an association between *Dlgap2* and AD phenotypes at the variant, gene and protein expression, and methylation levels. Lower cortical *DLGAP2* expression is observed in AD and is associated with more plaques and tangles at autopsy and faster cognitive decline. Results will inform future studies aimed at investigating the cross-species role of *Dlgap2* in regulating cognitive decline and highlight the benefit of using genetically diverse mice to prioritize novel candidates.

INTRODUCTION

Aging is the leading risk factor for a number of disorders, including dementias such as Alzheimer's disease. The mechanisms that underlie healthy aging—particularly, the cognitive as-

pects—remain poorly understood. Research suggests that genetics play a significant role in determining an individual's susceptibility or resilience to cognitive decline and dementia (Harris and Deary 2011; Ridge et al., 2013). Identification of precise genetic factors involved would provide insight into



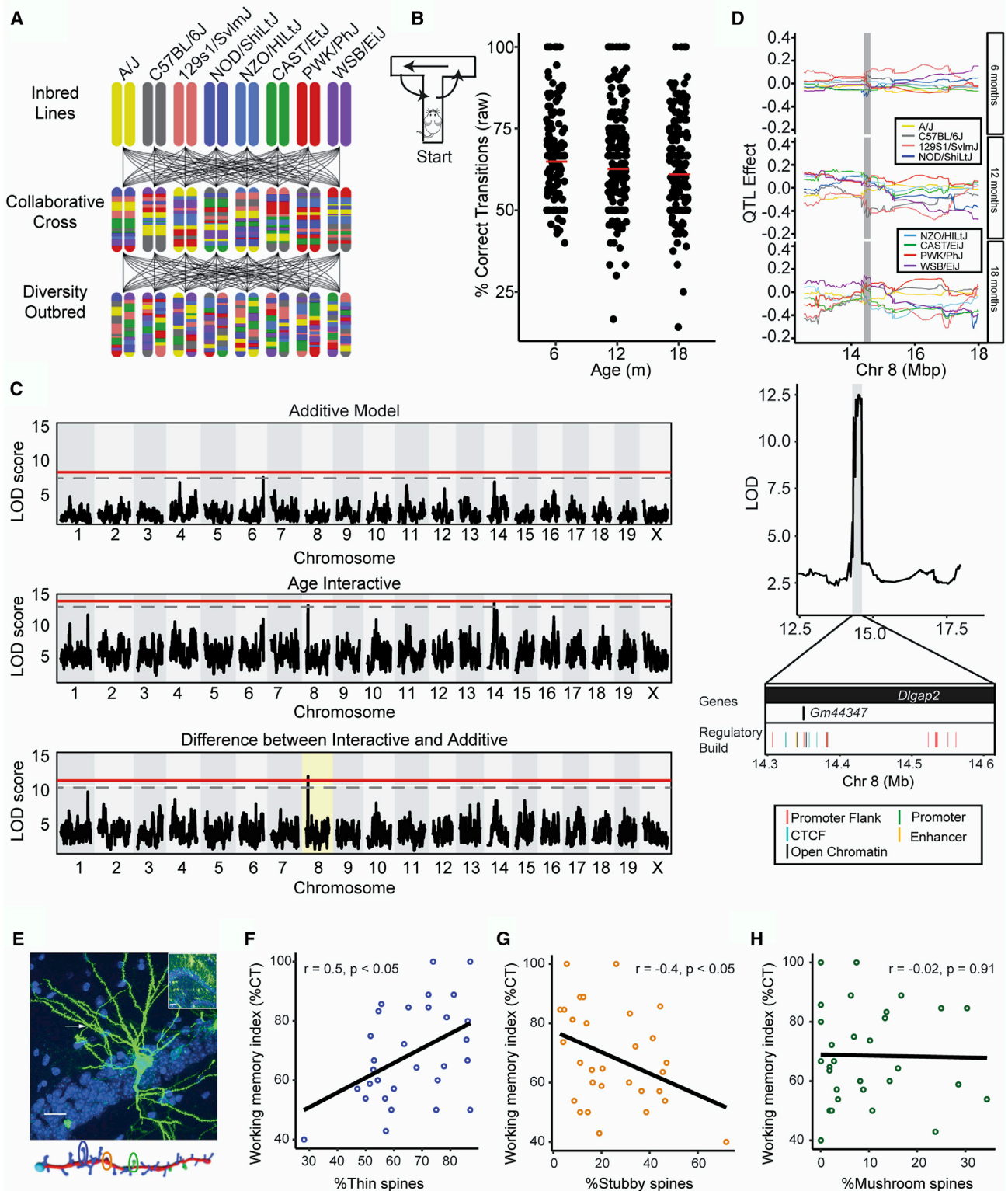


Figure 1. *Dlgap2* Mediates Cognitive Function across the Lifespan in DO Mice

(A) Diversity Outbred (DO) mice are a genetically diverse population derived from 8 parental lines, segregating for a total of 40 million single nucleotide polymorphisms (SNPs).

(legend continued on next page)

mechanisms underlying increased susceptibility and uncover therapeutic targets.

The mouse represents a critical resource to identify genetic factors influencing complex traits due to well-defined genetic backgrounds, well-controlled environmental conditions, and lower sample size requirements for genetic mapping than human populations. Recent efforts to expand the genetic resources available in the mouse have resulted in the development of the Diversity Outbred (DO) panel (Churchill et al., 2012; Logan et al., 2013), which is derived from an 8-parent population segregating approximately 40 million variants (Srivastava et al., 2017). The resulting offspring provide precision and power for genetic analysis of complex traits such as cognitive decline in aging.

Here, we perform a large-scale, cross-sectional evaluation of cognitive performance in the DO population aged 6 to 18 months and identify a single protein-coding positional candidate (disk-associated large protein 2, *Dlgap2*) likely mediating observed age-related decline. Across a subset of DO mice, we find that morphologic variation among dendritic spine populations significantly correlates with cognitive outcomes. As *Dlgap2* is a critical component of spines (Jiang-Xie et al., 2014), this finding provides an avenue for future mechanistic investigation into the observed association between *Dlgap2* and cognitive decline. Finally, we demonstrate that *Dlgap2* is associated with cognitive decline and Alzheimer's dementia (AD) in diverse human populations. Results highlight the utility of the mouse to (1) inform studies in human patients and (2) enable prioritization of genes and variants for further study.

RESULTS

Dlgap2 Mediates Cognitive Longevity in DO Mice

To identify genes involved in regulating the maintenance of cognitive function during aging, working memory was evaluated on the T-maze (Wenk, 2001) at 6, 12, or 18 months in 487 DO mice (Figure 1A). Working memory declined with age, $F(2, 484) = 2.8$, $p = 0.03$, one-tailed (Figure 1B). No effect of sex was observed on working memory performance, $F(1, 484) = 0.02$, $p = 0.90$. To identify genetic factors regulating working memory, we next performed genetic mapping. A quantitative trait locus (QTL) on chromosome 8 (chr8) (Figure 1C) that interacted with age to mediate working memory performance across the lifespan (LOD = 12.5, 1.5 LOD interval = 14.3–14.6 Mb, $p < 0.05$) was identified. Allelic coefficient plots demonstrate that, at 6 months of age, the non-obese diabetic (NOD) background contributes a lower working memory score, while the 129 and

B6 backgrounds contribute higher working memory scores (Figure 1D, top). Age interactions with this locus were largely driven by NOD, B6, and 129 at 12 months of age (Figure 1D, top; Figures S1A and S1B). We also see age interactions across the QTL haplotype region (Figure S1C). A single protein-coding gene, *Dlgap2*, is located within the QTL interval (Figure 1D, bottom), highlighting *Dlgap2* as the most likely positional candidate mediating working memory decline as a function of aging. SNP association tests within the QTL region using the most up-to-date Sanger sequencing information identified one high-confidence SNP and a single structural variant that differed between NOD and 129 within the intronic regions of the *Dlgap2* gene (Figure S1D).

Dlgap2 is a critical component of the postsynaptic density involved in regulating synaptic function and dendritic spine morphology (Li et al., 2017). Given studies linking structural alterations in dendritic spine morphology with age-related changes in cognitive function (Dickstein et al., 2013; Dumitriu et al., 2010; Boros et al., 2019), we measured the number and functional subtypes of spines in the hippocampus in a subset of DO mice at 6, 12, or 18 months of age (Figure 1E). We observed no changes in total spine density or distribution of spine type (thin, stubby, or mushroom; Table S1) with age. Neither spine density nor spine type correlated with cognitive outcomes at 6 or 12 months of age (Figure S2). However, by 18 months, there was a significant correlation between both the percentage of thin and stubby spines and working memory performance (Figures 1F–1H), suggesting that maintenance of high numbers of thin spines combined with lower numbers of stubby spines is beneficial for maintaining cognitive function during aging (Dumitriu et al., 2010).

Genetic Variants in the DLGAP2 Region Are Associated with AD

We next sought to test the translational relevance of this finding by evaluating the association of *DLGAP2* with clinically diagnosed dementia in human populations. We evaluated SNPs within the *DLGAP2* region (± 50 kb) within published and pending genome-wide association studies (GWASs) of clinical Alzheimer's disease. Among individuals with European ancestry (Jansen et al., 2019), one locus just downstream of *DLGAP2* was associated with AD: top SNP, rs2957061; $p = 3.6 \times 10^{-5}$; $\beta = -0.02$; odds ratio (OR) = 0.98; Figure S3A, Table S2). Among African American individuals, a locus within *DLGAP2* was associated with AD: top SNP, chr8:1316870; minor allele frequency (MAF) = 0.01; $p = 9.2 \times 10^{-5}$; $\beta = -0.86$, OR = 0.42; Figures 2A and S3B; Table S3).

(B) Working memory was assessed on the T-maze at 6, 12, or 18 months across 487 DO mice (6 months, 66 female mice [F]/67 male mice [M]; 12 months, 102 F/96 M; and 18 months, 76 F/80 M), and a significant effect of age was observed; one-way ANOVA, $F(2, 484) = 2.8$, $p = 0.03$, one-tailed. Red line represents the mean of displayed data.

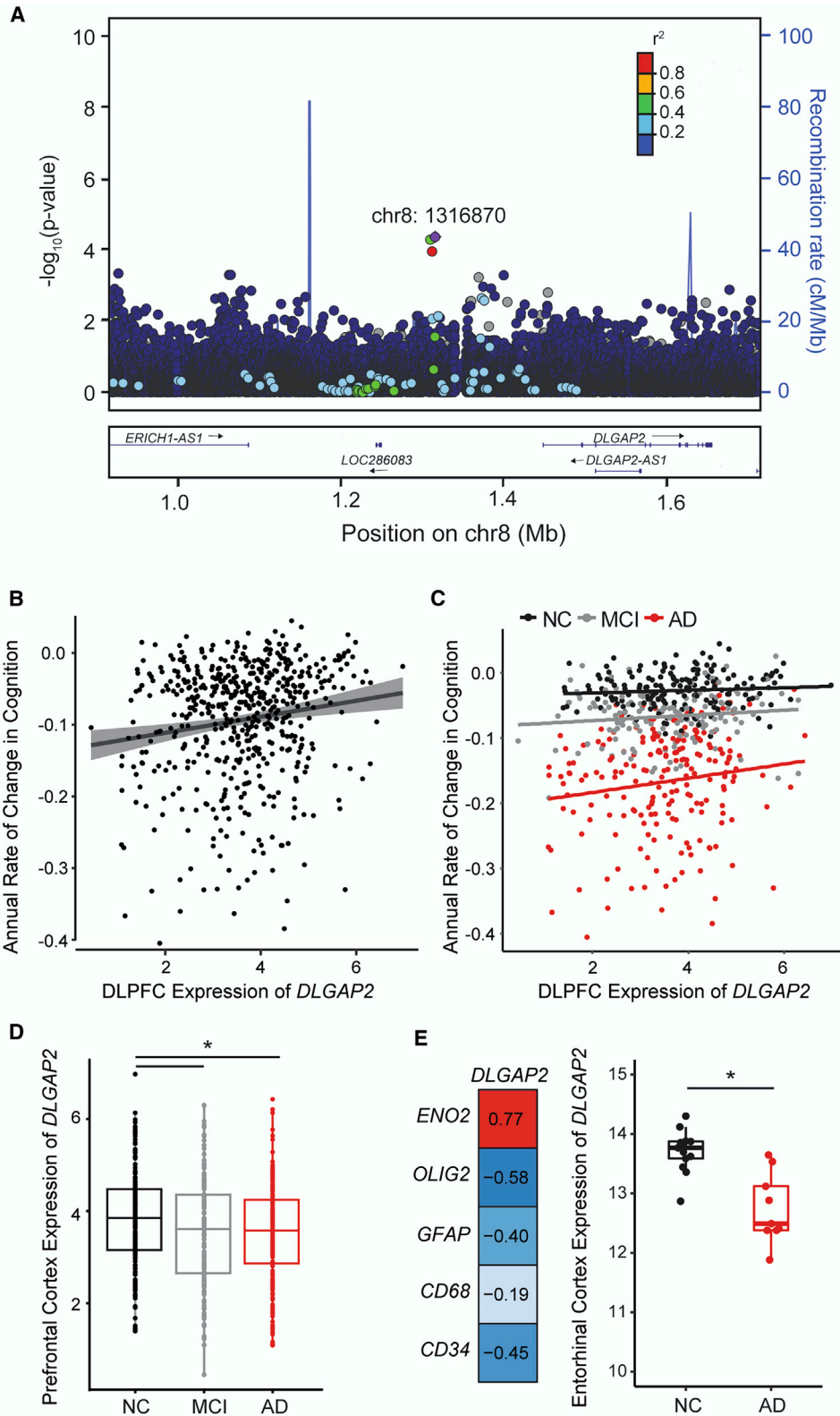
(C) A quantitative trait locus (QTL) on chr8 was identified that significantly interacted with age to mediate working memory performance across the lifespan (LOD = 12.5; 1.5 LOD interval = 14.3–14.6 Mb). Dashed line indicates permutation-based cutoff of suggestive QTL, $p = 0.20$. Red line indicates permutation-based cutoff for significant QTL, $p = 0.05$.

(D) Top: coefficient plots indicated according to the color key by founder allele illustrate the impact of each allele on working memory phenotype at 6, 12, and 18 months of age. Bottom: a single protein-coding gene, *Dlgap2*, is located within the QTL interval, along with a number of regulatory elements.

(E) Spine number and morphology were assessed in CA1 hippocampal pyramidal neurons. Scale bar, 10 μ m.

(F and G) Across 18-month-old DO mice, significant correlations between (F) working memory function and percentage of thin spines and (G) percentage of stubby spines was observed.

(H) No association between percentage of mushroom spines and working memory was observed.



(legend on next page)

A previous GWAS (White et al., 2017) reported that rs34130287C, a SNP within the first intron of *DLGAP2*, was suggestively associated with worse residual cognition ($p = 4.0 \times 10^{-6}$), a trait that quantified the gap between observed and predicted cognitive performance after regressing out the effect of neuropathology. *DLGAP2* was not pursued as a potential candidate because NCBI and Ensembl annotations, at the time of the prior report, did not include rs34130287C within *DLGAP2*. However, as of February 2019, current annotations place this SNP within *DLGAP2*. Using the same dataset and methods as initially reported (White et al., 2017), we observed a significant relationship between the overall methylation pattern of the *DLGAP2* region in the dorsolateral prefrontal cortex (DLPFC) and residual cognition ($p = 0.038$; Figure S3C). As methylation at the *DLGAP2* locus has been shown to influence *Dlgap2* expression in mouse (Chertkow-Deutsher et al., 2010), we hypothesize that the effect of this locus on cognitive function is mediated by alterations in *Dlgap2* expression in the DLPFC.

Expression of *DLGAP2* Is Associated with Cognitive Decline in Human Populations

We next sought to test this hypothesis by evaluating the association of *DLGAP2* with cognitive function and dementia in human populations. Across the Religious Orders Study and the Rush Memory and Aging Project (ROS/MAP), lower levels of *DLGAP2* mRNA in the DLPFC of post-mortem human brain tissue were associated with poorer cognitive performance at the final visit prior to death ($\beta = 0.10$, $p = 0.01$) and faster cognitive decline over all study visits ($\beta = 0.01$, $p = 0.002$; Figure 2B). This relationship was strongest among individuals with clinically diagnosed AD (Figure 2C). When assessing protein levels of *DLGAP2* measured with tandem mass tag mass spectrometry (Johnson et al., 2020), we observed a consistent finding with lower levels of *DLGAP2* protein associated with a faster rate of cognitive decline ($\beta = 0.29$, $p < 0.001$; Figure S3D).

DLGAP2 Is Differentially Expressed in Brains of Those with Cognitive Impairment

To assess differences in *DLGAP2* expression during various stages of cognitive impairment, we evaluated DLPFC mRNA expression of *DLGAP2* across ROS/MAP. Those with mild cognitive impairment (MCI) and clinically diagnosed AD had lower levels of expression compared to patients with normal cognition, $F(2, 528) = 4.4$, $p = 0.01$ (Figure 2D). A similar decrease of *DLGAP2* was observed in two independent datasets covering

5 brain regions (Table S4), strengthening our confidence in these findings. As *DLGAP2* is a component of synapses (Li et al., 2017) and highly correlated with expression of the neuronal marker *ENO2* (Figure 2E, left), it is possible that this decrease of *DLGAP2* is due to neurodegeneration that occurs in MCI and Alzheimer's disease. However, when considering only neuronal expression data from laser-capture microdissected neurons (Liang et al., 2008) to control for number of neurons evaluated, a significant decrease in *DLGAP2* remained (Figure 2E, right). This suggests that reduced *DLGAP2* occurs independent of frank neurodegeneration. While not associated with neurodegeneration, we next evaluated whether *DLGAP2* was associated with other neuropathological hallmarks of Alzheimer's disease measured with immunohistochemistry (IHC). Lower levels of *DLGAP2* were associated with greater β -amyloid load in the DLPFC ($\beta = -0.13$, $p = 0.002$). Similarly, lower levels of *DLGAP2* were associated with more neurofibrillary tangles in the DLPFC ($\beta = -0.11$, $p = 0.02$). No associations were observed with non-Alzheimer neuropathologies (Table S5; p values > 0.10).

DISCUSSION

Utility of DO Mice for Cross-Species Analyses

Despite the recent increase in availability and accessibility of genomic technologies, our understanding of the genetic mechanisms underlying complex traits remains poor. This is due, in part, to the difficulty in assigning causality to GWAS hits, a number of which occur in non-coding regions of the genome (Zhang and Lupski 2015). For example, the two loci highlighted here (Figures 2A and S3A) fall within complex genomic regions, making the biological mechanism driving the observed associations difficult to interpret. However, by combining these results with studies performed in the mouse, we not only identify *Dlgap2* as a potential causal gene in the region but also highlight structural plasticity and modification of spine type (Figures 1E–1H) as a mechanism putatively involved in modifying cognitive decline.

An additional factor complicating the identification of disease-causative genes using GWAS is a lack of statistical power, particularly in under-represented populations where sample size is relatively limited (Popejoy and Fullerton 2016). As a result, population-specific genetic mechanisms underlying diseases, and treatments that may prevent or cure them, remain undiscovered. To better inform population-specific analyses, mouse studies offer a powerful way to prioritize candidates. In

Figure 2. *DLGAP2* Is Associated with Cognitive Function and Alzheimer's Disease in Diverse Human Populations

(A) An SNP located at chr8: 1316870 (MAF = 0.01) was modestly associated with AD within a GWAS of African American individuals ($p = 9.2 \times 10^{-5}$). Current Ensembl annotation (as of February 2019, release 95; data not shown) places this SNP within the first intron of *DLGAP2*.
 (B) Across the ROS/MAP cohort, higher levels of *DLGAP2* in the dorsolateral prefrontal cortex (DLPFC) were associated with slower annual cognitive decline ($\beta = 0.01$, $p = 0.002$).
 (C) This association was strongest among patients clinically diagnosed with AD. Normal cognition (NC): $n = 180$, $\beta = 0.02$, $p = 0.43$; mild cognitive impairment (MCI): $n = 148$, $\beta = 0.04$, $p = 0.18$; AD: $n = 203$, $\beta = 0.08$, $p = 0.16$.
 (D) *DLGAP2* expression was significantly lower in the DLPFC of participants diagnosed with either MCI or clinical AD relative to NC, $F(2, 528) = 4.4$, $p = 0.01$.
 (E) Left: correlation of *DLGAP2* and cell-type-specific markers *ENO2* (neurons), *OLIG2* (oligodendrocytes), *GFAP* (astrocytes), *CD68* (microglia), and *CD34* (endothelial cells) as measured by RNA expression from DLPFC tissue across the ROS/MAP cohort. Right: expression of *DLGAP2* is decreased specifically in neurons from AD patients, as measured by RNA expression from laser-capture microdissected neurons from Liang et al. (2008); $p < 0.05$. Boxes encompass the 25th to 75th percentile with whiskers indicating 10th and 90th percentiles. Median lines are indicated within each box.

particular, the DO population provides an advantage over previous genetically diverse resources, including a higher degree of genetic diversity and smaller haplotype blocks, leading to more precise genomic mapping (Churchill et al., 2012). A caveat to this increased genetic diversity is the large number of allelic combinations present at any given locus. Although the present study was not sufficiently powered to estimate all heterozygous allelic combinations driving the effects, we were still able to identify founder effects in an eight-state additive model. By doing so, our mapping strategy nominated only one protein coding gene with well-known functions in regulating synaptic throughput, structure, and function (Jiang-Xie et al., 2014; Chertkow-Deutsher et al., 2010), highlighting the importance of this biological pathway to working memory. Although it is possible that these variants play a role in distal gene regulation, other sources of evidence supported our decision to move forward with *DLGAP2* as a top candidate for tests in human cohorts. This was based on combining our interactive mapping result highlighting *Dlgap2*, biological priors (Jiang-Xie et al., 2014), and our finding that variation in spine type is correlated with memory outcomes in aging DO mice that is consistent with findings in human studies (Boros et al., 2017). Overall, candidate genes nominated by studies in the DO have the potential to greatly contribute to the understanding of mechanisms underlying complex traits in both mouse and humans.

Dlgap2 and Cognitive Decline

Here, we show that reduced *Dlgap2* is associated with faster cognitive decline, AD and disease diagnosis, and increased neuropathology in humans across multiple brain regions and independent datasets. We also provide evidence that *DLGAP2* protein abundance in brain is associated with cognitive decline. Mutant mice that lack *Dlgap2*, a post-synaptic density scaffolding protein, show impaired initial reversal learning, deficits in synaptic communication, and reduced dendritic spine density (Jiang-Xie et al., 2014). Spine loss correlates more strongly to cognitive decline in Alzheimer's disease than the classical neuropathological hallmarks (Dorostkar et al., 2015; Boros et al., 2017; DeKosky and Scheff 1990; Terry et al., 1991). However, mechanisms underlying this loss of spines are still poorly understood. Work here suggests aging mouse models—at least the DO population, in particular—may provide an important experimental system in which to begin to understand mechanisms contributing to spine loss and cognitive dysfunction in human populations. Notably, the spine phenotypes that correlate to working memory in our DO population mimic the increase in thin spine density and simultaneous reduction in stubby spines observed exclusively in patients that exhibited cognitive resistance to Alzheimer's disease pathology (Boros et al., 2017, 2019). As we know, genotype at *Dlgap2* plays an important role in regulating cognitive decline in the DO population (Figure 1D), and *Dlgap2* critically regulates spine number and morphology (Jiang-Xie et al., 2014). Therefore, we hypothesize that *Dlgap2* may act as a potential driver of cognitive decline and later transition to dementia via its role in mediating spine-related phenotypes. This hypothesis will need to be experimentally tested, although the work here provides an important starting point for future mechanistic studies focused

on elucidating the role of *Dlgap2* in cognitive decline across species.

Conclusions and Future Directions

In summary, the work here identifies *Dlgap2* as a potential mediator of cognitive decline in both mouse and humans and highlights the benefit of using genetically diverse mouse populations to inform mechanistic studies and identify novel candidates involved in complex human disease. Future studies will investigate the role of identified variants, precise molecular mechanisms involved in mediating cognitive decline, and the utility of *Dlgap2* as a therapeutic target to promote healthy brain aging.

STAR★METHODS

Detailed methods are provided in the online version of this paper and include the following:

- KEY RESOURCES TABLE
- RESOURCE AVAILABILITY
 - Lead Contact
 - Materials Availability
 - Data and Code Availability
- EXPERIMENTAL MODEL AND SUBJECT DETAILS
- METHOD DETAILS
 - Behavioral testing
 - Genetic mapping
 - Spine analysis
 - Human study participants
 - African American GWAS Analysis: Sample Characteristics
 - Genotype quality control and imputation
 - Association analysis
 - Differential gene expression analysis in humans
 - Gene expression associations with neuropathologies of age-related disease
 - Analysis of DLPFC gene expression associations with longitudinal cognition in humans
 - Analysis of DNA methylation in DLPFC
- QUANTIFICATION AND STATISTICAL ANALYSIS

SUPPLEMENTAL INFORMATION

Supplemental Information can be found online at <https://doi.org/10.1016/j.celrep.2020.108091>.

ACKNOWLEDGMENTS

This work was supported by National Institute on Aging grants R01AG054180, R01AG057914, and RF1AG063755 (to C.C.K.), K01AG049164 and R01AG059716 (to T.J.H.), and F31AG050357 (to S.M.N.); The Jackson Laboratory Nathan Shock Center on Aging grant P30AG038070 (to G.C. and L.P.); the Healthspan Core (to E.J.C.); and NIH grants P50 DA 039841 (to E.J.C.), P30AG10161, R01AG15819, R01AG17917, and R01AG36042 (to J.A.S. and D.A.B.), R01AG061800 and R01AG054719 (to J.H.H.), U01AG61356 (to P.L.D.J. and D.A.B.), R01AG061800 and R01AG054719 (to J.H.H.), and U01AG61356 (to P.L.D.J. and D.A.B.). C.R. was supported by NIH/NIA grants R01AG064614, 1RF1AG054080, 1U01AG052410, P50 AG08702, and U01AG032984. N.T.S. was supported by NIH grants U01AG061357, RF1AG057471, RF1AG057470, and RF1AG062181. The Genotype-Tissue Expression (GTEx) Project was supported by the Common Fund of the Office

of the Director of the National Institutes of Health and by the NCI, NHGRI, NHLBI, NIDA, NIMH, and NINDS.

The data used for the analyses described in this article were obtained from the GTEx Portal on 4/25/2019 and/or dbGaP: phs000424.vN.pN on 4/25/19 (<https://gtexportal.org/home/gene/DLGAP2>). The results published here are in whole or in part based on data obtained from the AMP-AD Knowledge Portal (<https://adknowledgeportal.synapse.org/>). The AMP-AD Knowledge Portal is a platform for accessing data, analyses, and tools generated by the AMP-AD Target Discovery Program and other programs supported by the National Institute on Aging to enable open-science practices and accelerate translational learning. The data, analyses, and tools are shared early in the research cycle without a publication embargo on secondary use. Data are available for general research use according to the requirements for data access and data attribution (<https://adknowledgeportal.synapse.org/#/DataAccess/Instructions>). ROS/MAP resources can be requested at <https://www.radc.rush.edu>.

Data from Alzheimer's Disease Genetics Consortium (ADGC) were appropriately downloaded from the dbGaP database (dbGaP: phs000372.v1.p1). We acknowledge the contributions of the members of the ADGC.

AUTHOR CONTRIBUTIONS

C.C.K. conceived of, and led, the integrative cross-species analyses, with critical input from T.J.H., N.H., and E.J.C. G.C. and L.P. generated and maintained the aging colony for cross-sectional mouse experiments. E.J.C. and L.C.A. designed, oversaw, and implemented the behavioral phenotyping procedures and neuroanatomical procedures. A.R.O., S.M.N., N.H., D.M.G., J.A.B., and C.C.K. performed the genetic analysis of behavior and anatomical analyses and generated figures. T.J.H., L.D., E.R.M., and B.W.K. performed the human genetic analyses and contributed to critical manuscript revisions. H.-S.Y. performed the DLPFC methylation association analyses and revised the manuscript. D.A.B., J.A.S., P.L.D.J., C.R., and C.C.W. provided clinical, genomic, epigenomic, transcriptomic, and neuropathologic data; assisted with analyses and interpretation of results; and provided critical revisions to the manuscript. J.H.H. also assisted with interpretation of anatomical results and provided critical revisions to the manuscript. S.M.N., A.R.O., L.D., N.H., and C.C.K. drafted the manuscript. All authors contributed to subsequent versions and have approved of the final submission.

DECLARATION OF INTERESTS

C.C.K. and S.M.N. have filed a related patent application. The other authors declare no competing interests.

Received: May 16, 2019

Revised: February 10, 2020

Accepted: August 7, 2020

Published: September 1, 2020

REFERENCES

Allen, M., Carrasquillo, M.M., Funk, C., Heavner, B.D., Zou, F., Younkin, C.S., Burgess, J.D., Chai, H.S., Crook, J., Eddy, J.A., et al. (2016). Human whole genome genotype and transcriptome data for Alzheimer's and other neurodegenerative diseases. *Sci. Data* 3, 160089.

Allen, M., Wang, X., Burgess, J.D., Watzlawik, J., Serie, D.J., Younkin, C.S., Nguyen, T., Malphrus, K.G., Lincoln, S., Carrasquillo, M.M., et al. (2018). Conserved brain myelination networks are altered in Alzheimer's and other neurodegenerative diseases. *Alzheimers Dement.* 14, 352–366.

Amador-Ortiz, C., Lin, W.L., Ahmed, Z., Personett, D., Davies, P., Duara, R., Graff-Radford, N.R., Hutton, M.L., and Dickson, D.W. (2007). TDP-43 immunoreactivity in hippocampal sclerosis and Alzheimer's disease. *Ann. Neurol.* 61, 435–445.

Arvanitakis, Z., Capuano, A.W., Leurgans, S.E., Buchman, A.S., Bennett, D.A., and Schneider, J.A. (2017). The Relationship of Cerebral Vessel Pathology to Brain Microinfarcts. *Brain Pathol.* 27, 77–85.

Bennett, D.A., Schneider, J.A., Arvanitakis, Z., and Wilson, R.S. (2012a). Overview and findings from the religious orders study. *Curr. Alzheimer Res.* 9, 628–645.

Bennett, D.A., Schneider, J.A., Buchman, A.S., Barnes, L.L., Boyle, P.A., and Wilson, R.S. (2012b). Overview and findings from the rush Memory and Aging Project. *Curr. Alzheimer Res.* 9, 646–663.

Bennett, D.A., Buchman, A.S., Boyle, P.A., Barnes, L.L., Wilson, R.S., and Schneider, J.A. (2018). Religious Orders Study and Rush Memory and Aging Project. *J. Alzheimers Dis.* 64 (s7), S161–S189.

Boros, B.D., Greathouse, K.M., Gentry, E.G., Curtis, K.A., Birchall, E.L., Gearing, M., and Herskowitz, J.H. (2017). Dendritic spines provide cognitive resilience against Alzheimer's disease. *Ann. Neurol.* 82, 602–614.

Boros, B.D., Greathouse, K.M., Gearing, M., and Herskowitz, J.H. (2019). Dendritic spine remodeling accompanies Alzheimer's disease pathology and genetic susceptibility in cognitively normal aging. *Neurobiol. Aging* 73, 92–103.

Boyle, P.A., Yu, L., Nag, S., Leurgans, S., Wilson, R.S., Bennett, D.A., and Schneider, J.A. (2015). Cerebral amyloid angiopathy and cognitive outcomes in community-based older persons. *Neurology* 85, 1930–1936.

Broman, K.W., and Sen, S. (2009). *A Guide to QTL Mapping with R/qtl* (Springer).

Broman, K.W., Gatti, D.M., Simecek, P., Furlotte, N.A., Prins, P., Sen, S., Yandell, B.S., and Churchill, G.A. (2019). R/qtl2: Software for Mapping Quantitative Trait Loci with High-Dimensional Data and Multiparent Populations. *Genetics* 211, 495–502.

Buchman, A.S., Leurgans, S.E., Nag, S., Bennett, D.A., and Schneider, J.A. (2011). Cerebrovascular disease pathology and parkinsonian signs in old age. *Stroke* 42, 3183–3189.

Chen, M.H., and Yang, Q. (2010). GWAF: an R package for genome-wide association analyses with family data. *Bioinformatics* 26, 580–581.

Chertkow-Deutsher, Y., Cohen, H., Klein, E., and Ben-Shachar, D. (2010). DNA methylation in vulnerability to post-traumatic stress in rats: evidence for the role of the post-synaptic density protein Dlgap2. *Int. J. Neuropsychopharmacol.* 13, 347–359.

Churchill, G.A., Gatti, D.M., Munger, S.C., and Svenson, K.L. (2012). The Diversity Outbred mouse population. *Mamm. Genome* 23, 713–718.

De Jager, P.L., Srivastava, G., Lunnon, K., Burgess, J., Schalkwyk, L.C., Yu, L., Eaton, M.L., Keenan, B.T., Ernst, J., McCabe, C., et al. (2014). Alzheimer's disease: early alterations in brain DNA methylation at ANK1, BIN1, RHBDF2 and other loci. *Nat. Neurosci.* 17, 1156–1163.

DeKosky, S.T., and Scheff, S.W. (1990). Synapse loss in frontal cortex biopsies in Alzheimer's disease: correlation with cognitive severity. *Ann. Neurol.* 27, 457–464.

Dickstein, D.L., Weaver, C.M., Luebke, J.I., and Hof, P.R. (2013). Dendritic spine changes associated with normal aging. *Neuroscience* 251, 21–32.

Dorostkar, M.M., Zou, C., Blazquez-Llorca, L., and Herms, J. (2015). Analyzing dendritic spine pathology in Alzheimer's disease: problems and opportunities. *Acta Neuropathol.* 130, 1–19.

Dumitriu, D., Hao, J., Hara, Y., Kaufmann, J., Janssen, W.G., Lou, W., Rapp, P.R., and Morrison, J.H. (2010). Selective changes in thin spine density and morphology in monkey prefrontal cortex correlate with aging-related cognitive impairment. *J. Neurosci.* 30, 7507–7515.

Gatti, D.M., Svenson, K.L., Shabalin, A., Wu, L.Y., Valdar, W., Simecek, P., Goodwin, N., Cheng, R., Pomp, D., Palmer, A., et al. (2014). Quantitative trait locus mapping methods for diversity outbred mice. *G3 (Bethesda)* 4, 1623–1633.

Harris, S.E., and Deary, I.J. (2011). The genetics of cognitive ability and cognitive ageing in healthy older people. *Trends Cogn. Sci.* 15, 388–394.

Jansen, I.E., Savage, J.E., Watanabe, K., Bryois, J., Williams, D.M., Steinberg, S., Sealock, J., Karlsson, I.K., Hägg, S., Athanasiu, L., et al. (2019). Genome-wide meta-analysis identifies new loci and functional pathways influencing Alzheimer's disease risk. *Nat. Genet.* 51, 404–413.

- Jiang-Xie, L.F., Liao, H.M., Chen, C.H., Chen, Y.T., Ho, S.Y., Lu, D.H., Lee, L.J., Liou, H.H., Fu, W.M., and Gau, S.S. (2014). Autism-associated gene *Dlgap2* mutant mice demonstrate exacerbated aggressive behaviors and orbitofrontal cortex deficits. *Mol. Autism* 5, 32.
- Johnson, E.C.B., Dammer, E.B., Duong, D.M., Ping, L., Zhou, M., Yin, L., Higinbotham, L.A., Guajardo, A., White, B., Troncoso, J.C., et al. (2020). Large-scale proteomic analysis of Alzheimer's disease brain and cerebrospinal fluid reveals early changes in energy metabolism associated with microglia and astrocyte activation. *Nat. Med.* 26, 769–780.
- Li, J., Zhang, W., Yang, H., Howrigan, D.P., Wilkinson, B., Souaiaia, T., Evgrafov, O.V., Genovese, G., Clementel, V.A., Tudor, J.C., et al. (2017). Spatiotemporal profile of postsynaptic interactomes integrates components of complex brain disorders. *Nat. Neurosci.* 20, 1150–1161.
- Liang, W.S., Reiman, E.M., Valla, J., Duncley, T., Beach, T.G., Grover, A., Niedzielko, T.L., Schneider, L.E., Mastroeni, D., Caselli, R., et al. (2008). Alzheimer's disease is associated with reduced expression of energy metabolism genes in posterior cingulate neurons. *Proc. Natl. Acad. Sci. USA* 105, 4441–4446.
- Lim, A.S., Srivastava, G.P., Yu, L., Chibnik, L.B., Xu, J., Buchman, A.S., Schneider, J.A., Myers, A.J., Bennett, D.A., and De Jager, P.L. (2014). 24-hour rhythms of DNA methylation and their relation with rhythms of RNA expression in the human dorsolateral prefrontal cortex. *PLoS Genet.* 10, e1004792.
- Logan, R.W., Robledo, R.F., Recla, J.M., Philip, V.M., Bubier, J.A., Jay, J.J., Harwood, C., Wilcox, T., Gatti, D.M., Bult, C.J., et al. (2013). High-precision genetic mapping of behavioral traits in the diversity outbred mouse population. *Genes Brain Behav.* 12, 424–437.
- Popejoy, A.B., and Fullerton, S.M. (2016). Genomics is failing on diversity. *Nature* 538, 161–164.
- Reitz, C., Jun, G., Naj, A., Rajbhandary, R., Vardarajan, B.N., Wang, L.S., Valadares, O., Lin, C.F., Larson, E.B., Graff-Radford, N.R., et al.; Alzheimer Disease Genetics Consortium (2013). Variants in the ATP-binding cassette transporter (*ABCA7*), apolipoprotein E ϵ 4, and the risk of late-onset Alzheimer disease in African Americans. *JAMA* 309, 1483–1492.
- Ridge, P.G., Mukherjee, S., Crane, P.K., and Kauwe, J.S.; Alzheimer's Disease Genetics Consortium (2013). Alzheimer's disease: analyzing the missing heritability. *PLoS ONE* 8, e79771.
- Schindelin, J., Arganda-Carreras, I., Frise, E., Kaynig, V., Longair, M., Pietzsch, T., Preibisch, S., Rueden, C., Saalfeld, S., Schmid, B., et al. (2012). Fiji: an open-source platform for biological-image analysis. *Nat. Methods* 9, 676–682.
- Schneider, J.A., Wilson, R.S., Cochran, E.J., Bienias, J.L., Arnold, S.E., Evans, D.A., and Bennett, D.A. (2003). Relation of cerebral infarctions to dementia and cognitive function in older persons. *Neurology* 60, 1082–1088.
- Schneider, J.A., Boyle, P.A., Arvanitakis, Z., Bienias, J.L., and Bennett, D.A. (2007). Subcortical infarcts, Alzheimer's disease pathology, and memory function in older persons. *Ann. Neurol.* 62, 59–66.
- Schneider, J.A., Arvanitakis, Z., Yu, L., Boyle, P.A., Leurgans, S.E., and Bennett, D.A. (2012). Cognitive impairment, decline and fluctuations in older community-dwelling subjects with Lewy bodies. *Brain* 135, 3005–3014.
- Srivastava, A., Morgan, A.P., Najarian, M.L., Sarsani, V.K., Sigmon, J.S., Shorter, J.R., Kashfeen, A., McMullan, R.C., Williams, L.H., Giusti-Rodríguez, P., et al. (2017). Genomes of the Mouse Collaborative Cross. *Genetics* 206, 537–556.
- Terry, R.D., Masliah, E., Salmon, D.P., Butters, N., DeTeresa, R., Hill, R., Hansen, L.A., and Katzman, R. (1991). Physical basis of cognitive alterations in Alzheimer's disease: synapse loss is the major correlate of cognitive impairment. *Ann. Neurol.* 30, 572–580.
- Wang, M., Beckmann, N.D., Roussos, P., Wang, E., Zhou, X., Wang, Q., Ming, C., Neff, R., Ma, W., Fullard, J.F., et al. (2018). The Mount Sinai cohort of large-scale genomic, transcriptomic and proteomic data in Alzheimer's disease. *Sci. Data* 5, 180185.
- Wenk, G.L. (2001). Assessment of spatial memory using the T maze. *Curr. Protoc. Neurosci.*, Chapter 8: Unit 8.5B.
- White, C.C., Yang, H.S., Yu, L., Chibnik, L.B., Dawe, R.J., Yang, J., Klein, H.U., Felsky, D., Ramos-Miguel, A., Arfanakis, K., et al. (2017). Identification of genes associated with dissociation of cognitive performance and neuropathological burden: Multistep analysis of genetic, epigenetic, and transcriptional data. *PLoS Med.* 14, e1002287.
- Willer, C.J., Li, Y., and Abecasis, G.R. (2010). METAL: fast and efficient meta-analysis of genomewide association scans. *Bioinformatics* 26, 2190–2191.
- Wilson, R.S., Boyle, P.A., Yu, L., Barnes, L.L., Sytsma, J., Buchman, A.S., Bennett, D.A., and Schneider, J.A. (2015). Temporal course and pathologic basis of unawareness of memory loss in dementia. *Neurology* 85, 984–991.
- Zhang, F., and Lupski, J.R. (2015). Non-coding genetic variants in human disease. *Hum. Mol. Genet.* 24 (R1), R102–R110.

STAR★METHODS

KEY RESOURCES TABLE

REAGENT or RESOURCE	SOURCE	IDENTIFIER
Critical Commercial Assays		
RNeasy Lipid Tissue Mini Kit	QIAGEN	Cat#74804
Illumina TotalPrep RNA Amplification Kit	Thermo Fisher Scientific	Cat# AMIL1791
Deposited Data		
Accelerating Medicines Partnership Alzheimer's Disease project	https://www.synapse.org/#!/Synapse:syn14237651	syn14237651
MayoRNaseq study	https://www.synapse.org/#!/Synapse:syn5550404	syn5550404
Mount Sinai Brain Bank (MSBB) study	https://adknowledgeportal.synapse.org/Explore/Studies/DetailsPage?Study=syn3159438	syn3159438
dbGaP	https://www.ncbi.nlm.nih.gov/gap/	phs000372.v1.p1
GeneNetwork	http://gn1.genenetwork.org/webqtl/main.py?FormID=sharinginfo&GN_AccessionId=233	Accession GN233
African American GWAS	https://www.niagads.org/datasets/ng00100	ID NG00100
Experimental Models: Organisms/Strains		
Mouse: Diversity Outbred (J:DO)	The Jackson Laboratory	JAX # 009376
Software and Algorithms		
R/qtI2	Broman et al., 2019	https://kbroman.org/qtI2/
Ethovision	Noldus Information Technology	https://www.noldus.com/
Fiji-ImageJ	Schindelin et al., 2012	https://imagej.net/Fiji
Imaris	Oxford Instruments	https://imaris.oxinst.com/
METAL	Willer et al., 2010	https://sph.umich.edu/csg/abecasis/metal/
BeadStudio	Illumina	https://www.illumina.com/
GWAF	Chen and Yang, 2010	http://www2.uaem.mx/r-mirror/web/packages/GWAF/GWAF.pdf

RESOURCE AVAILABILITY

Lead Contact

Further information and requests for resources and reagents should be directed to and will be fulfilled by the Lead Contact, Catherine C. Kaczorowski (catherine.kaczorowski@jax.org).

Materials Availability

Diversity outbred mice used in this study are currently available from the Jackson Laboratory (<https://www.jax.org/strain/009376>), JAX#009376. This study did not generate new unique reagents.

Data and Code Availability

The accession number for the summary-level data from a harmonized differential gene expression analysis completed by the Accelerating Medicines Partnership Alzheimer's Disease project is AMP-AD Knowledge portal:syn14237651 (<https://www.synapse.org/#!/Synapse:syn14237651>).

The accession number for the data from the MayoRNaseq study is:AMP-AD Knowledge portal: syn5550404 (<https://www.synapse.org/#!/Synapse:syn5550404>). The accession number for the Mount Sinai Brain Bank (MSBB) study is AMP-AD Knowledge Portal: syn3159438 (<https://adknowledgeportal.synapse.org/Explore/Studies/DetailsPage?Study=syn3159438>). The accession number for the RNA expression from laser-captured micro-dissected neurons is [GeneNetwork.org](http://gn1.genenetwork.org): GN Accession #233

(http://gn1.genenetwork.org/webqtl/main.py?FormID=sharinginfo&GN_AccessionId=233). The accession number for the summary statistics for African American GWAS is NIAGADS: NG00100 (<https://www.niagads.org/datasets/ng00100>).

EXPERIMENTAL MODEL AND SUBJECT DETAILS

Diversity Outbred (J:DO) mice were obtained from The Jackson Laboratory via the Nathan Shock Center of Excellence in the Basic Biology of Aging. All mice were part of a cross-sectional phenotyping project in which independent cohorts of mice were timed for nearly simultaneous testing of 6, 12 and 18 month old mice to avoid repeated testing. The sample sizes for each group were as follows: 6 m = 66F/67M, 12 m = 102F/96M, 18 m = 76F/80M. Mice were genotyped using the MegaMUGA array (GeneSeek, Lincoln, Nebraska) and genotype probabilities estimated using R/DOQTL (Gatti et al., 2014). Mice were housed in duplex polycarbonate cages on ventilated racks providing 99.997% HEPA filtered air to each cage in a climate-controlled room under a standard 12:12 light-dark cycle (lights on at 0600 h). Singly housed mice were provided with enrichment in the form of a Shepherd Shack. All experiments were performed during the light phase of the light/dark cycle. Pine bedding was changed weekly and mice were provided ad-libitum access to food (NIH31 5K52 chow, LabDiet/PMI Nutrition, St. Louis, MO) and acidified water. All procedures and protocols were approved by The Jackson Laboratory Animal Care and Use Committee, and were conducted in compliance with the National Institutes of Health Guidelines for the Care and Use of Laboratory Animals.

METHOD DETAILS

Behavioral testing

Behavioral testing was performed during the light phase of a 12:12 light/dark cycle. The spontaneous continuous alternation T-maze test was performed using the Med Associates

(St. Albans, VT) mouse maze (MED-TMMN) with 3 arms placed at 90 degrees to one another on an octagonal hub. The maze was situated in the center of a 10 ft. x 10 ft. room. Large (approximately 24 inch) distinct visual cues comprising geometric shapes made from self-adhesive vinyl were on the surrounding walls. Mice were transferred from the housing room to the testing room via a wheeled cart and allowed to habituate for at least 60 minutes prior to testing. Mice were removed from the cage one at a time for the maze trial and returned to the home cage after testing. Mice were placed into an enclosed arm of the T-maze and after 10 s the guillotine door was lifted and the mouse was allowed to explore freely for the remainder of the 5 min trial. The trials were recorded using a single overhead camera and videos were tracked automatically using Noldus Ethovision V7 (Wageningen, NL) to determine time spent in each arm. The center point of the mouse was used to determine mouse position at a rate of 29.9 frames per second. Post-processing to calculate number of transitions and the percent of correct alternations were calculated using the Sequence Analysis Tool (SAT), an Excel macro provided by Noldus Ethovision designed to calculate zone transitions and analyze sequences of arms visited. In a correct alternation mice visit all three arms before reentering a previously visited arm. Errors include repeat visits to a single arm within the previous three arms visited, or failure to visit all three arms. Mice who avoid an arm completely over the duration of the trial are omitted from analysis. Time spent in each arm, number of transitions, and the percent of correct alternations were calculated.

Genetic mapping

Genetic mapping was conducted using R/qtl2 (qtl2geno, qtl2scan, and qtl2plot packages) to perform single quantitative trait loci (QTL) scans with sex and age as covariates (Broman et al., 2019). To identify QTL that interact with age and play a role in regulating cognitive decline, age was also included as an interactive covariate. Results (i.e., LOD scores) from the additive scans were subtracted from results from the interactive scans to identify QTL that uniquely interacted with age and were not present in the additive model. Permutation tests were used in each case to evaluate significance. For simple additive and interactive scans, 1000 standard permutations were performed. For evaluating significance for the interactive-minus-additive scans (Figure 1C, bottom), permutations were performed as follows: First, genotypes and phenotypes are permuted identically across interactive and additive models. Genome-wide scans for each model were performed 1000 times, with genotype/phenotype randomization occurring differently for each permutation, but kept the same between additive/interactive scans. For each permutation the additive LOD scores were subtracted from the interactive; the maximum LOD score of these differentiated peaks was recorded. From the distribution of 1000 maximum LOD scores, the score in the 95th percentile ($\alpha = 0.05$) was selected and used as the significance threshold for interactive-additive difference QTL map. QTL that exhibit a higher difference score than this significance threshold are said to significantly interact with age to determine working memory performance (Broman and Sen, 2009; Broman et al., 2019). These QTL represent particularly interesting loci, as genotype at these locations putatively interact with age to mediate decline over time, rather than just confer high cognitive reserve and good cognitive performance across the lifespan (Broman and Sen, 2009).

Spine analysis

At the completion of all phenotyping including physiological testing, mice were decapitated to preserve brain tissue and brains removed. The brain was hemisected, and the right hippocampus was saved for RNA analysis and the left hemisphere was used for diolistic labeling and dendritic spine analyses. The brain was hemisected using 2 single edge stainless steel razor blades. Blades are cleaned between mice and replaced every ~4 mice.

The left hemisphere was placed in ~5 mL 4% PFA in PBS for 1 hr. After 1 hr., the sample was moved into 4 mL 1x PBS at room temperature and stored at 4°C overnight. Within several days the brains were sliced in the coronal plane in the brain matrix and ~150 μm sections were obtained using a vibratome. The sections were placed in PBS in 6 well plates. A Helios gene gun was used to label the sections with Dil-coated tungsten beads. The samples were left in the dark at room temperature overnight. After 24 hours the sections were post-fixed in 4% PFA for one hour. The slices were then counter-stained with DAPI and mounted on slides using Dako anti-fade mounting medium and the slides were stored at 4°C in the dark until confocal imaging was completed. A Leica SP5 or SP8 confocal microscope was used to obtain a 20x z stack at ~1 μm step size of the whole neuron and a 63x glycerol immersion z stack of secondary dendritic branches for spine analysis. One pyramidal neuron of the CA1 region of the hippocampus was imaged for each mouse. To be analyzed, dendrites must have been a minimum of ten micrometers in length. The analysis was completed by a blind observer, with no knowledge of the mouse's age group or performance on behavioral tests.

The image analysis consisted of quantifying dendrite length, spine count, spine density, and spine morphology using Fiji ImageJ (Schindelin et al., 2012) and the FilamentTracer module in Imaris software. The Classify Spines feature was used to categorize spine types.

Human study participants

To validate the translation relevance of candidate genes associated with memory performance in DO mice, data and summary results were obtained from a number of well-defined studies of cognitive aging and Alzheimer's dementia (AD). First, gene level results were assessed leveraging data from two cohort studies of cognitive aging, The Religious Orders Study (ROS) and The Rush Memory and Aging Project (MAP). Both studies enrolled participants free of dementia who agreed to annual clinical evaluations and brain donation at death (Bennett et al., 2012a, 2012b, 2018). Informed consent and an Anatomical Gift Act for organ donation was obtained from all participants, participants signed a repository consent for resource sharing, and all research adhered to individual Institutional Review Board (IRB)-approved protocols.

Second, data from the MayoRNaseq study (<https://www.synapse.org/#!Synapse:syn5550404>) and the Mount Sinai Brain Bank (MSBB) study (<https://adknowledgeportal.synapse.org/Explore/Studies/DetailsPage?Study=syn3159438>) were leveraged for replication of differential expression results from ROS/MAP. In the Mayo study, post-mortem samples were collected from the temporal cortex and cerebellum, as previously described (Allen et al., 2016, 2018). In the MSBB study, post-mortem samples were collected from the inferior frontal gyrus, frontal pole, parahippocampal gyrus, and superior temporal gyrus as previously described (Wang et al., 2018).

Finally, we leveraged summary statistics from a recently published GWAS of AD among individuals of European Ancestry (Jansen et al., 2019) and in African American participants (B.W.K., M. Schmidt, H.-U. Klein, A.C. Naj, K.L. Hamilton-Nelson, and C.R., unpublished data). Given the most up-to-date African American GWAS of AD, additional details are provided below. All human analyses were completed using RStudio (version 1.1.453; <https://rstudio.com/>) with R version 3.3.1.

African American GWAS Analysis: Sample Characteristics

A GWAS meta-analysis was completed leveraging data from 8084 African American individuals who were 60 years of age or older (2838 cases, 5246 controls, 69% female). Clinical diagnosis of AD was established using standard procedures within each study site, protocols have been published previously (Reitz et al., 2013).

Genotype quality control and imputation

Standard quality control for genotype and sample-level data was conducted individually for each dataset. Single-nucleotide polymorphisms with call rates less than 98% or not in Hardy-Weinberg equilibrium ($p < 10^{-6}$ in controls) were excluded. Individuals with non-African American ancestry according to principal components (PCs) analysis of ancestry informative markers were excluded, as were participants whose reported sex differed from the sex assignment determined by analysis of the X chromosome SNPs. Latent relatedness among participants within and across the case-control cohorts was identified by the estimated proportion of alleles (π) shared identical by descent (IBD). One participant from each duplicate pair ($\pi > 0.95$) or relative pair ($0.4 \leq \pi < 0.95$) was included in the sample used for association analyses, prioritizing based on non-missing disease status and then higher SNP call rate. After genotype quality control, all datasets were individually phased and SNPs were imputed with the African Genome Resource (AGR) using the Sanger Imputation Service (<https://www.sanger.ac.uk/tool/sanger-imputation-service/>). Common variants (minor allele frequency [MAF] ≥ 0.01) with imputation quality score < 0.4 , rare variants (MAF < 0.01) with imputation quality < 0.7 , and variants present in less than 30% of AD cases and 30% of controls across all datasets were excluded from downstream analyses. Human genome build GRCh37 was used.

Association analysis

Single variant association analysis was performed on genotype dosages using an additive model adjusting for age, sex, and PCs. For case-control datasets, we employed logistic regression, while family-based datasets used generalized estimating equations (GEE) as implemented in GWAF (Chen and Yang 2010). Within-study results were meta-analyzed using an inverse-variance based model with genomic control as implemented in METAL (Willer et al., 2010).

Differential gene expression analysis in humans

In ROS/MAP, RNA expression levels were obtained from frozen, manually dissected dorsolateral prefrontal cortex (DLPFC) tissue (Lim et al., 2014). Isolation of RNA was performed using the RNeasy lipid tissue kit (QIAGEN, Valencia, CA) and it was reverse transcribed using the Illumina® TotalPrep RNA Amplification Kit from Ambion (Illumina, San Diego, CA). Following sequencing, processing of the expression signals was performed using the BeadStudio software suite (Illumina, San Diego, CA). Standard normalization and quality control methods were then employed (Lim et al., 2014). Differential expression of *DLGAP2* between individuals with AD and individuals with normal cognition prior to death was assessed using linear regression, covarying for age at death and sex. Summary-level data from a harmonized differential gene expression analysis completed by the Accelerating Medicines Partnership Alzheimer's Disease project (<https://www.synapse.org/#!Synapse:syn14237651>) was used for replication in Mayo and MSSM. Additionally, RNA expression from laser-captured micro-dissected neurons described previously (Liang et al., 2008) was utilized via GeneNetwork.org (GN Accession: #233) to assess cell-type specific changes of *DLGAP2* expression.

Gene expression associations with neuropathologies of age-related disease

Neuropathological measures available in ROS/MAP have been described in detail previously (Bennett et al., 2012a, 2012b). For the present analyses, we utilized previously collected measures of phosphorylated tau and β -amyloid quantified with immunohistochemistry (IHC). The percentage of area occupied by β -amyloid or tau averaged across 8 brain regions (hippocampus, angular gyrus, and entorhinal, midfrontal, inferior temporal, calcarine, anterior cingulate, and superior frontal cortices). Associations between *DLGAP2* mRNA levels and β -amyloid plaques and tau tangles were assessed using linear regression covarying for age at death and sex. Outcomes were square-root-transformed to better approximate a normal distribution.

Additional semiquantitative measures included TDP-43 pathology, cerebral amyloid angiopathy (CAA), atherosclerosis, arteriosclerosis, gross infarctions, micro infarctions, and Lewy bodies. Details of the measurement and quantification for these methods have been published previously but are also summarized here. Six brain regions (amygdala, hippocampus CA1, dentate gyrus, entorhinal, midtemporal, and midfrontal cortices) were stained with monoclonal phosphorylated TDP-43 antibodies to obtain a score from 0 (indicating absence of pathology) to 4 (indicating presence of pathology in all regions) (Amador-Ortiz et al., 2007). CAA was measured in the midfrontal, midtemporal, parietal and calcarine cortices and the burden of pathology was summarized with a score from 0 (no deposition) to 3 (severe deposition) across the regions (Boyle et al., 2015). Circle of Willis vessels were visually inspected for atherosclerosis which was quantified by a score from 0 (no significant atherosclerosis) to 3 (over half had atherosclerosis or at least one had 75% occlusion or both) (Arvanitakis et al., 2017). Severity of arteriosclerosis was classified into 4 levels, 0 indicating no histological changes and 3 indicating severe changes (Buchman et al., 2011). Nine regions (midfrontal, midtemporal, entorhinal, hippocampal, inferior parietal and anterior cingulate cortices, anterior basal ganglia, thalamus, and midbrain) were examined to determine the presence or absence of gross and microinfarctions. Gross infarctions were identified by visual inspection and confirmed histologically. Micro infarctions were identified by inspection of 6 μ m hematoxylin/eosin stained paraffin-embedded sections of each region (Arvanitakis et al., 2017; Schneider et al., 2003, 2007). Lewy body disease was measured in sections from eight of the nine brain regions mentioned above (not the thalamus) by α -synuclein immunostaining and coded as 0 (not present), 1 (nigral-predominant), 2 (limbic-type), or 3 (neocortical-type) (Schneider et al., 2012). All associations with these outcomes were assessed using binary logistic regression or proportional odds models covarying for age at death and sex.

Analysis of DLPFC gene expression associations with longitudinal cognition in humans

Cognitive function was quantified into a single composite measure generated by averaging the z-scores of 17 cognitive tests that spanned 5 domains of cognitive function (episodic, semantic, and working memory, perceptual orientation, and perceptual speed) (Wilson et al., 2015). For this measurement, a negative score is indicative of worse cognitive performance over time. Longitudinal associations between *DLGAP2* expression and global cognition in ROS/MAP were tested using mixed-effects regression. Age at death, sex, gene expression level, latency to death (time between final visit and death), interval (years between neuropsychological visit and final visit prior to death), and an interval x gene expression interaction term were considered fixed effects. The intercept and interval were additionally entered as random effects in the model.

Analysis of DNA methylation in DLPFC

A residual cognition score was calculated as previously described (White et al., 2017), in which lower scores represent lower cognitive performance than predicted given the level of neuropathology present in the brain. Specifically, residual cognition was captured by regressing out the effects of cerebral pathologies (including Alzheimer's disease pathology, cerebrovascular pathologies, Lewy bodies, and hippocampal sclerosis) and demographic characteristics (age at death, sex, years of education, and study cohort) from global cognitive performance proximate to death.

DLPFC DNA methylation was measured as previously described (De Jager et al., 2014). For the present analysis we defined the *DLGAP2* region as the chromosomal region that includes the gene and its flanking 100 kb at the 5' and 3' ends, according to the NCBI *Homo sapiens* annotation release 109 and Ensemble release 95 (hg19: Chr 8, from 777021 bp through 1756642 bp). There were 798 CpGs within this region. In 648 ROS/MAP participants with non-missing data, we assessed the association between residual cognition and the overall methylation pattern of the *DLGAP2* region using the previously described method (White et al., 2017). In

brief, we first assessed the association between each CpG (independent variable) and residual cognition (dependent variable), controlling for technical variables, and derive an observed test statistic from the p values using Fisher's method:

$$\text{Test statistic} = - \sum \log_{10} p_{\text{CpG}}$$

Then, by permuting the dependent variable (residual cognition), we ran 10,000 simulations to derive 10,000 simulated test statistics. Finally, we calculated the empiric p value for the observed test statistic based on the simulated test statistics, to assess whether the overall association between *DLGAP2* region's methylation pattern and residual cognition deviates from the simulated null distribution.

QUANTIFICATION AND STATISTICAL ANALYSIS

Statistical analyses were performed as described in the [STAR Methods](#). Analyses were performed in R, METAL and GWAF. Behavioral data were checked for normality with Q-Q plots and Shapiro Wilk testing; data were log-transformed to ensure normality for statistical analysis and QTL mapping. Relevant statistical analyses and n sizes are reported in figure legends and [Results](#) section. Data values reported in both the main text and figure legends are given as mean \pm standard error of the mean unless otherwise stated.

Supplemental Information

Cross-Species Analyses Identify *Dlgap2*

as a Regulator of Age-Related

Cognitive Decline and Alzheimer's Dementia

Andrew R. Ouellette, Sarah M. Neuner, Logan Dumitrescu, Laura C. Anderson, Daniel M. Gatti, Emily R. Mahoney, Jason A. Bubier, Gary Churchill, Luanne Peters, Matthew J. Huentelman, Jeremy H. Herskowitz, Hyun-Sik Yang, Alexandra N. Smith, Christiane Reitz, Brian W. Kunkle, Charles C. White, Philip L. De Jager, Julie A. Schneider, David A. Bennett, Nicholas T. Seyfried, Alzheimer's Disease Genetics Consortium, Elissa J. Chesler, Niran Hadad, Timothy J. Hohman, and Catherine C. Kaczorowski

Supplemental Tables

Table S1. Related to Figure 1: Distribution of spine type by age. Spine density and percentage of each spine type observed at either 6 months (m), 12 m, or 18 m in a subset of DO mice (n = 55). No effect of age was observed on total spine density [ANOVA $F(2, 52) = 1.0$, $p = 0.4$] or on distribution of spine type [Chi-square test; $\chi^2(4, n = 55) = 2.4$, $p = 0.6$].

Spine Type	6 m	12 m	18 m
Stubby	31.2	28.9	24.6
Thin	63.6	64.7	65.6
Mushroom	5.2	6.4	9.8
Total Density (# spines/10 μm)	9.3	10.0	11.3

Table S2. Related to Figure 2: Top GWAS hits within the *DLGAP2* region from Jansen et al. (2019). Single nucleotide polymorphisms within the *DLGAP2* region ($\pm 50\text{Kb}$) were evaluated for association with clinical Alzheimer’s dementia using published data from a cohort of individuals with European ancestry (Jansen et al. 2019). Under direction, “-” indicates protective effect, “+” indicates risk, “?” indicates not present.

SNP	P-value	N_{sum}	N_{eff}	Dir	MAF	Beta	SE
rs2957061	3.59E-05	71639	71639	?-?-	0.44	-0.022	0.005
rs2972183	3.66E-05	71639	71639	?-?-	0.44	-0.022	0.005
rs4433174	4.40E-05	71639	71639	?-?-	0.43	-0.022	0.005
rs2957059	4.42E-05	71639	71639	?-?-	0.44	-0.022	0.005
rs2972180	5.53E-05	71639	71639	?-?-	0.42	-0.022	0.005
rs2977182	7.67E-05	71639	71639	?+?+	0.48	0.021	0.005
rs2957060	1.07E-04	71639	71639	?+?+	0.48	0.020	0.005
rs73490628	2.13E-04	403592	402286	??+-	0.021	0.029	0.008
rs56066830	3.40E-04	17477	17477	??+?	0.026	0.120	0.033
rs571506119	4.12E-04	386906	386906	??-?	0.0009	-0.132	0.037
rs139482790	4.83E-04	387096	387096	??+?	0.00009	0.413	0.118
rs145185101	5.04E-04	386879	386879	??+?	0.00049	0.178	0.051
rs550396507	5.71E-04	386548	386548	??+?	0.0017	0.095	0.028
rs571859582	5.71E-04	386549	386549	??+?	0.0017	0.096	0.028

Abbreviations: SNP: single nucleotide polymorphism, N_{sum}: total sample size, N_{eff}: effective sample size [= 4 / (1 / N_{cases} + 1 / N_{controls})], Dir: Directionality, MAF: Minor allele frequency, SE: standard error

Table S3. Related to Figure 2: Top 10 GWAS hits within the *DLGAP2* region from African American GWAS. Single nucleotide polymorphisms within the *DLGAP2* region (\pm 50Kb) were evaluated for association with clinical Alzheimer’s dementia using unpublished data from a cohort of individuals with African ancestry (Kunkle et al. 2019, pending submission). Under direction, “-” indicates protective effect of the minor allele compared to the major allele, “+” indicates risk, “?” indicates not present.

Variant	P-value	Dir	Beta	SE
8:1316870	9.19E-05	+-----?---???	-0.86	0.22
8:927728	0.0002	---+--?-----+	-0.15	0.04
8:1313008	0.0003	-+++++?+++???	0.80	0.22
8:936158	0.0003	---+-----?-	-0.50	0.14
8:855450	0.0004	+--+++++++--+	0.48	0.14
8:778641	0.0005	+++++++?--+	0.49	0.14
8:843935	0.0005	---+-----?+-	-0.49	0.14
8:772060	0.0005	+++++++?--+	0.49	0.14
8:1405507	0.0005	--+-----	-0.61	0.18
8:1685397	0.0006	+++++++?+++	0.33	0.10

Abbreviations: Dir: Directionality, SE: standard error

Table S4. Related to Figure 2: *DLGAP2* differential expression across brain regions. Differential expression analysis comparing expression of *DLGAP2* (Ensembl Gene ID: ENSG00000198010/HGNC symbol: Dlgap2) in Alzheimer’s dementia patients to controls (comparison: AD-Control in all cases) across multiple brain regions.

Tissue	LogFC	CI.L	CI.R	Av. Expr	T	P.value	Adj. P	β	Direction	Study
Cerebellum	-0.28	-0.47	-0.08	-1.24	-2.82	0.005	0.02	-2.58	Down	Mayo
Temporal Cortex	-0.33	-0.53	-0.14	-1.24	-3.33	0.0009	0.004	-1.19	Down	Mayo
Frontal Pole (BA10)	-0.02	-0.11	0.07	5.11	-0.43	0.66	0.88	-6.06	None	MSSM
Superior Temporal Gyrus (BA22)	-0.12	-0.23	-0.01	5.11	-2.22	0.03	0.16	-3.74	Down	MSSM
Parahippocampal Gyrus (BA36)	-0.23	-0.34	-0.12	5.11	-4.21	2.85E-05	0.004	2.13	Down	MSSM
Inferior Frontal Gyrus (BA 44)	-0.13	-0.23	-0.02	5.11	-2.34	0.02	0.20	-3.41	Down	MSSM

Abbreviations: LogFC: log fold change, CI: confidence interval, Av. Expr: average expression

Table S5. Related to Figure 2: Association between *DLGAP2* levels and non-Alzheimer’s disease neuropathology. DLPFC expression of *DLGAP2* was compared to semi-quantitative measures of non-Alzheimer’s pathology across the ROS/MAP cohort. All were assessed using binary logistic regression or proportional odds models covarying for age at death and sex.

Non-AD Neuropathology	Beta	SE	T	P-value
Cerebral Amyloid Angiopathy	-0.048	0.073	-0.662	0.51
Cerebral Atherosclerosis	0.005	0.072	0.067	0.95
Arteriolosclerosis	-0.045	0.069	-0.642	0.52
Lewy Bodies	-0.061	0.100	-0.614	0.54
Gross Infarctions (in Cortex)	-0.100	0.098	-1.022	0.31
Gross Infarctions (Anywhere)	-0.086	0.080	-1.073	0.28
Chronic Microinfarcts	-0.141	0.089	-1.592	0.11

Abbreviations: SE: standard error

Supplemental Figures

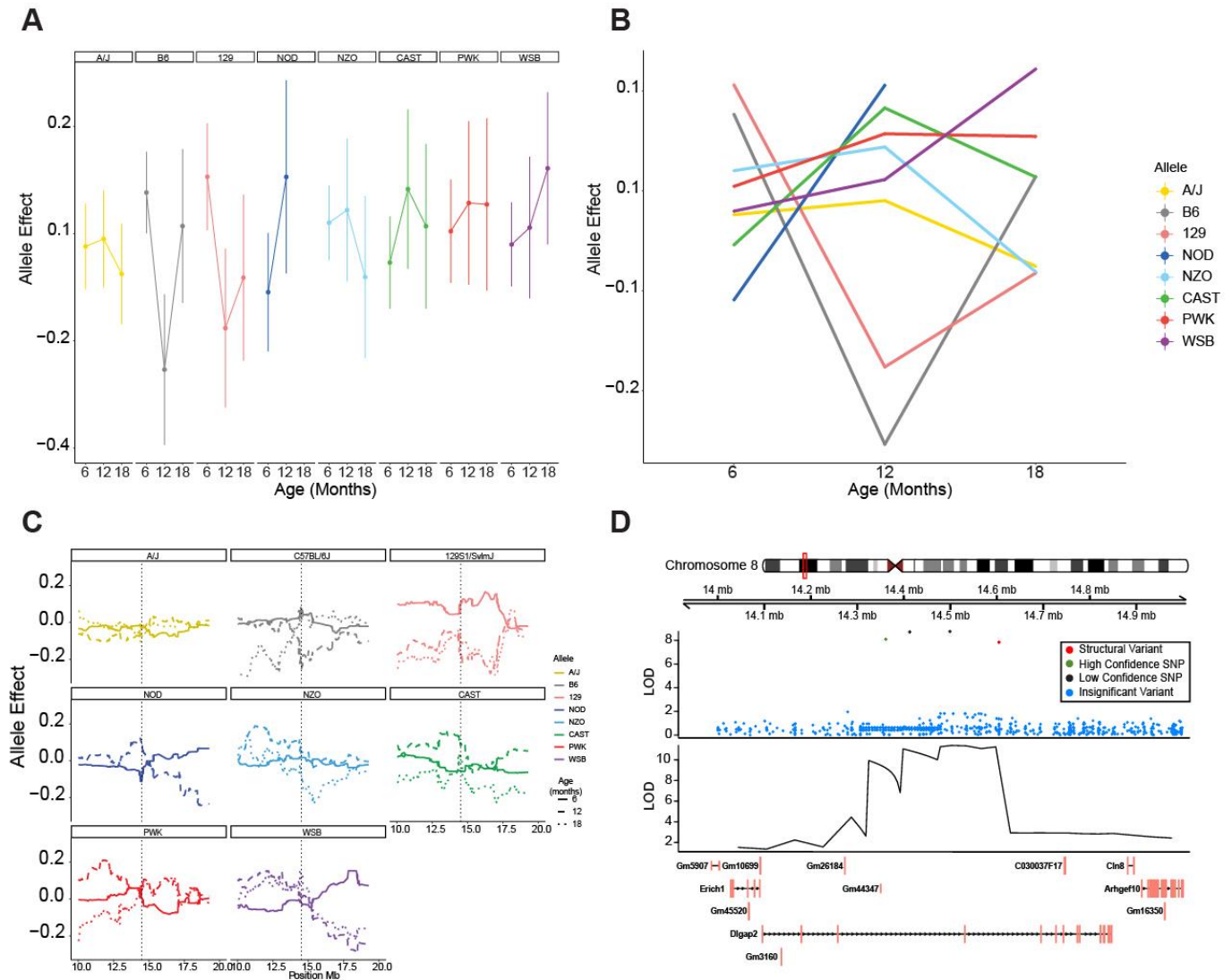
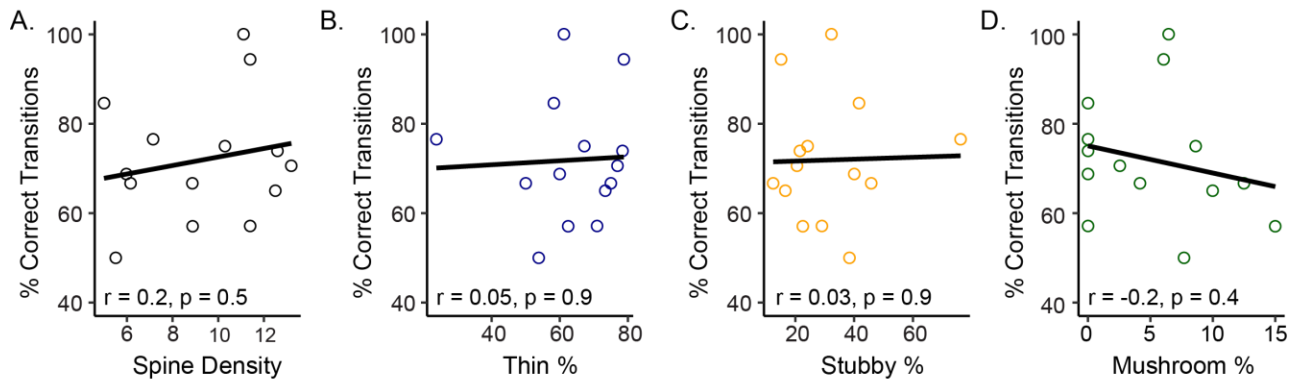


Figure S1. Related to Figure 1: Allele effect interactions with age and SNP association mapping at the *Dlgap2* QTL peak marker. A) Founder allele effect on working memory at the *Dlgap2* region separated by age group. B) Interaction plot demonstrating allele effect x age interactions for each founder allele. C) Founder allele effect on working memory at the *Dlgap2* haplotype region separated by founder allele and age. Dotted black line denotes the location of the QTL peak marker. D) SNP association mapping using variants segregating the diversity outbred population identified by Sanger revealed 3 significant intronic SNPs and 1 structural variant in the *Dlgap2* locus. The SNP at chr 8, 14.36131Mbp was high confidence, while the two SNPs positioned at chr 8, 14.41273 Mbp and 14.49918Mbp were noted as low confidence SNPs. The structural variant was noted as a deletion between position 14.604700Mbp and 14.604947Mbp that is private to NOD.

Spine Distribution - 6 months



Spine Distribution - 12 months

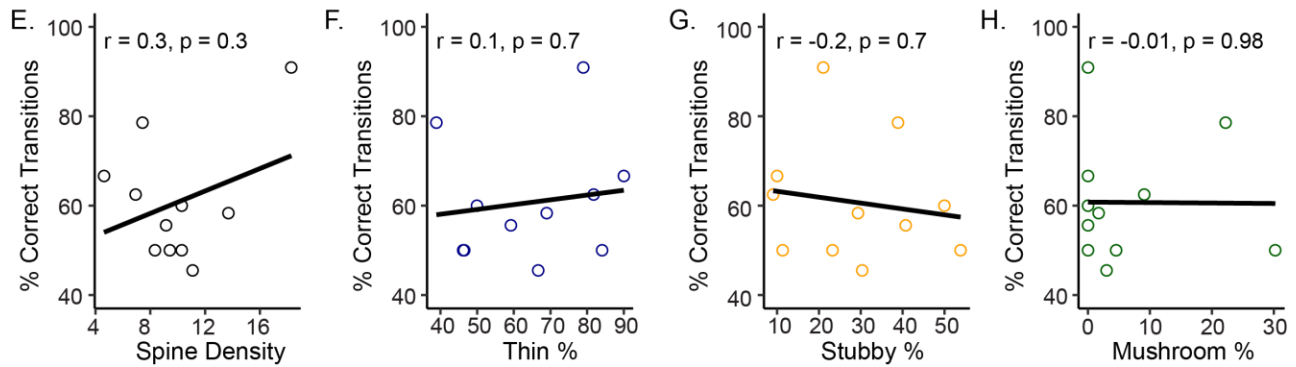


Figure S2. Related to Figure 1: Spine density or type does not correlate to working memory at either 6 or 12 months of age. A) Spine density (# spines/10 μm) across a subset of 6-month-old DO mice did not significantly correlate to working memory function as measured by percentage of correct transitions in the T-maze. Neither did B) percentage of thin spines, C) percentage of stubby spines, nor D) percentage of mushroom spines. E-H) No significant correlations were observed between the same measures at 12 months of age.

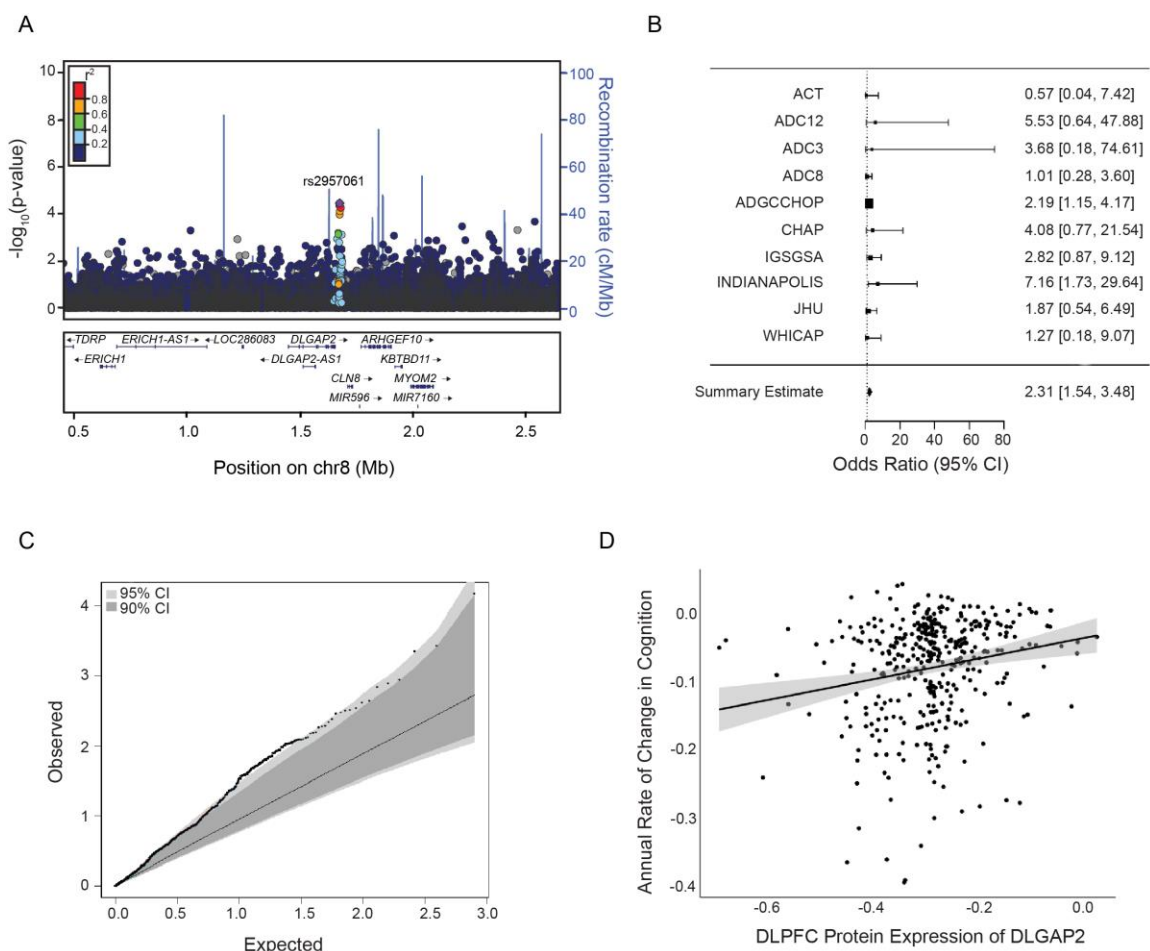


Figure S3. Related to Figure 2: *DLGAP2* SNP association, DNA methylation and protein expression in humans. A) Previously published GWAS data from individuals with European ancestry (Jansen et al. 2019) was used to evaluate the association between SNPs within the *Dlgap2* region (± 50 Kb) and clinical Alzheimer’s dementia. B) Across 10 datasets used in our meta-analysis, chr8:1316870 showed consistent association with increased risk for clinical Alzheimer’s dementia after adjustment for age, sex, and principal components of ancestry-informative markers. C) The observed association of each CpG within the *DLGAP2* region with residual cognition was plotted as a quantile-quantile plot, along with the confidence intervals (CI) derived from 10,000 simulated association statistics. Observed associations were stronger than simulated test results (Fisher’s method; $p=0.038$), indicating that the DNA methylation pattern from the *DLGAP2* region is associated with residual cognition. D) Across the ROS/MAP cohort, lower protein levels of DLGAP2 in the dorsolateral prefrontal cortex (DLPFC) were associated with higher annual cognitive decline ($\beta = 0.29$, $p = <0.001$).